Eur. Phys. J. D **43**, 125–128 (2007)
DOI: 10.1140/epjd/e2007-00054-4

THE EUROPEAN PHYSICAL JOURNAL D

Frontier orbitals analysis and density-functional energetics for metal-substituted fullerene $C_{58}Fe_2$

C. Tang[1,2], K. Deng[1,2,a], W. Tan[1,2], Y. Yuan[1,2], Y. Liu[1,2], J. Yang[2], and X. Wang[1]

[1] Department of Applied Physics, Nanjing University of Science and Technology, 210094 Nanjing Jiangsu, P.R. China
[2] Laboratory of Bond Selective Chemistry, University of Science and Technology of China, Hefei, 230026 Anhui, P.R. China

Received 23 July 2006 / Received in final form 30 October 2006
Published online 24 May 2007 –

Abstract. The formation mechanism, geometric structures, and electronic properties of a metal-substituted fullerene $C_{58}Fe_2$ have been studied using frontier orbital theory (FOT) and density functional theory (DFT). FOT predicts that two Fe atoms prefer to substitute the two carbons of a [6,6] double bond of C_{60} yielding a structure denoted as $C_{58}Fe_2$-3, which is different from the two equivalent substitution sites, i.e., the sites on the opposite of C_{60} cage or in the nearest neighboring sites of a pentagonal ring for $C_{58}X_2$ (X = N and B), and also different from the cross sites of a hexagonal ring for $C_{58}Si_2$. Five possible structures of $C_{58}Fe_2$ are optimized using DFT to see whether FOT works. The DFT calculations support the prediction of FOT. The Mulliken charge of Fe atom in $C_{58}Fe_2$-3 shows that the two Fe atoms of $C_{58}Fe_2$-3 lose 0.70 electron to the carbons of the cage, and the net spin populations of Fe atom indicate that each Fe atom has 1.11 μ_B magnetic moments, while each of the four nearest neighboring carbons has -0.064 μ_B magnetic moments. Thus, the two Fe atoms have ferromagnetic interaction with each other, and have weak antiferromagnetic interaction with their four nearest neighboring carbons, leaving 2.0 μ_B magnetic moments for the molecule.

PACS. 78.40.Ri Fullerenes and related materials – 73.22.-f Electronic structure of nanoscale materials: clusters, nanoparticles, nanotubes, and nanocrystals – 71.15.Mb Density functional theory, local density approximation, gradient and other corrections

1 Introduction

The doped fullerenes recently attracted special attention due to their intriguing properties and reactivity [1,2]. For example, it was found that C_{60} becomes a superconductor by doping alkali metals in the interstitial vacant sites for fcc C_{60} crystal [1] and the doped C_{70} exhibits the third-order optical nonlinearities [2]. Fullerenes are unique because they can be doped in several different ways, including: (1) trapped inside the hollow fullerene cage (endohedral), (2) located outside the cage (exohedral), and (3) incorporated hetero atoms into the fullerene network by replacement of carbon atoms (substitutional) [3]. Of particular interest is to study the possibility of controlling the electronic properties of fullerenes by incorporating appropriate impurity atoms into C_{60} network. Experimentally, Guo et al. [4] demonstrated that boron could be substitutionally doped into the fullerene cage to form $C_{60-x}B_x$ (x = 1 to 6). Yu et al. [5] reported the synthesis of nitrogen-substituted fullerenes such as $C_{59}N$ and $C_{58}N_2$. Kimura et al. [6] and Fye et al. [7] produced silicon-substituted carbon fullerenes. Recently, Billas et al. [8] reported the substitutionally doped fullerenes $C_{59}M$ and $C_{69}M$ (M = Fe, Ni, Rh, and Ir). The peak corresponding to $C_{58}M_2$ (M = Fe, Rh and Ir) has been observed in the photoionization mass spectrum of $C_{60-x}M_x$. Obviously, the assignment of the $C_{58}M_2$ (M = Fe, Rh and Ir) to substitutionally doped heterofullerenes would be tempting. According to the view of Schmalz et al. [9] that a cage appears to be the best candidate for the stable structures of a cluster with more than 30 carbon atoms. In addition, the cage structures of heterofullerenes such as $C_{58}X_2$ (X = Si, N, and B) [10–13] have been observed and isolated. Theoretically, Chen et al. [10] investigated the properties of $C_{68}B_2$ and $C_{68}N_2$. Kurita et al. [11] found that the closed-cage structures of $C_{58}X_2$ (X = N, B) were stable when the two X atoms were on the opposite sides of the cage or in the nearest neighboring sites of a pentagonal ring. On the other hand, Billas et al. [12,13] pointed out that the two Si atoms would be on the cross sites of a hexagonal ring for a stable closed-cage $C_{58}Si_2$. Therefore, it is possible that the $C_{58}Fe_2$ has a stable cage structure.

However, a theoretical study on the substitutionally doped $C_{58}Fe_2$ cage, to the best of our knowledge, has not yet been carried out so far. Thus we studied the substitution sites of two Fe atoms so as to explore the formation

[a] e-mail: kmdeng@mail.njust.edu.cn

mechanism, geometric structures and electronic properties of $C_{58}Fe_2$ in this paper. We describe our computational details in Section 2 and present our results and discussion in Section 3. Finally the conclusion is given in Section 4.

2 Computational details

All calculations are performed using generalized gradient approximation (GGA) [14] based on DFT [15]. The Becke-Lee-Yang-Parr (BLYP) correlation exchange function and DNP basis set are adopted for both Fe and carbon. BLYP function is the combination of the exchange function exploited by Becke [16] and the correlation function exploited by Lee, Yang and Parr [17]. The DNP basis set, comparable to Gaussian 6-31G** set, is the double numerical atomic orbitals augmented by polarization functions, i.e., functions with angular momentum one higher than that of the highest occupied orbital in the free atom. So the $1s$-$2p$, $3d$ wave functions for C, and $1s$-$4p$ wave functions for Fe are explicitly used. Electronic structure is obtained by solving the Kohn-Sham (KS) equations [18] self-consistently using the spin unrestricted scheme. Mulliken population analysis is used to obtain both the charge and net spin populations on each atom. Self-consistent field procedures are carried out with a convergence criterion of 10^{-6} a.u. on the energy and electron density. Geometry optimizations are performed using the Broyden-Fletcher-Goldfarb-Shanno (BFGS) algorithm [19] with a convergence criterion of 10^{-3} a.u. on the displacement and 10^{-5} a.u. on the energy.

3 Results and discussion

3.1 The formation mechanism of $C_{58}Fe_2$

Before calculation, we first explore the formation mechanism of $C_{58}Fe_2$ via the FOT [20]. We believe that the chemisorption of a molecule on the fullerene can be regarded as a process of chemical reaction between them to form another doped fullerene, namely:

$$C_{59}M + M_n \longrightarrow C_{59}M_{n+1}. \quad (1)$$

According to the FOT, when two reactant molecules approach, the interacting between the highest occupied molecular orbital (HOMO) of one molecule and the lowest unoccupied molecular orbital (LUMO) of the other should have close energies. When Branz et al. [21] reported that the condition for the substitution is that at least two metal atoms reside on the cage, and the initial fragmentation channel of the doped fullerenes is the loss of an MC molecule. So we assume that an iron dimer react with $C_{59}Fe$. While one Fe atom bonds to a carbon atom and leaves the cage in the form of a FeC molecule, the other Fe will fill the hole left by the missing carbon atom as a result of the chemical process.

Figure 1 schematically shows the frontier orbitals of $C_{59}Fe$ and Fe_2. One can easily see from the figure that

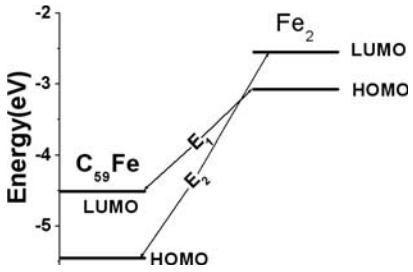

Fig. 1. The HOMO and LUMO of Fe_2 and $C_{59}Fe$.

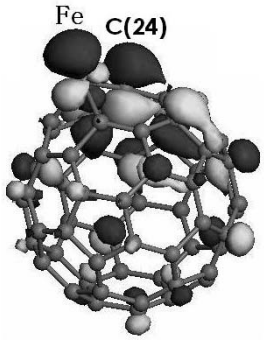

Fig. 2. The wave functions of the LUMO for $C_{59}Fe$.

the energy span E_1 between the LUMO of $C_{59}Fe$ and the HOMO of Fe_2 is much less than the energy span E_2 between the HOMO of $C_{59}Fe$ and the LUMO of Fe_2, so the action will occur mainly between the LUMO of $C_{59}Fe$ and the HOMO of Fe_2. On the other hand, we note from the FOT that the atom which has the most contribution to the LUMO of $C_{59}Fe$ will have the most possibility to interact with Fe atom. Figure 2 shows the wave function of the LUMO of $C_{59}Fe$, where the dark and light grays represent the negative and positive wave functions. It is obvious from the figure that the contribution from C(24) to the LUMO is the most, so we infer that the C(24) atom will interact and then form an externally doped fullerene. The Fe and C(24) in Figure 2 are the two atoms of a [6,6] double bond, the fusing bond of two hexagons. Therefore, the places of a [6,6] double bond of C_{60} are the favorable substituted sites for two Fe atoms to form $C_{58}Fe_2$ molecule.

The transformation process from an externally doped cage to a substitutionally doped cage, which is the second step in forming $C_{58}Fe_2$, can be suggested to occur along the following channel

$$C_{59}Fe_3 \longrightarrow C_{58}Fe_2 + FeC. \quad (2)$$

Combining equations (1) and (2), we obtain:

$$C_{59}Fe + Fe_2 \longrightarrow C_{58}Fe_2 + FeC. \quad (3)$$

3.2 The stability of $C_{58}Fe_2$

As shown above, the most possibly substituted site of Fe in $C_{59}Fe$ has been predicted by FOT, however, does FOT work? In order to check the reliability of FOT, we next

Table 1. The HOMO, LUMO, E_g and BE of C_{60}, $C_{59}Fe$, and five isomers of $C_{58}Fe_2$ with unit in eV.

Isomer	HOMO	LUMO	E_g	BE
C_{60}	–5.99	–4.33	1.66	423.20
$C_{59}Fe$	–5.45	–4.51	0.94	417.84
$C_{58}Fe_2$-1	–5.20	–4.77	0.43	412.43
$C_{58}Fe_2$-2	–4.67	–4.65	0.02	412.49
$C_{58}Fe_2$-3	–5.09	–4.37	0.72	412.98
$C_{58}Fe_2$-4	–5.16	–4.32	0.84	412.76
$C_{58}Fe_2$-5	–5.17	–4.35	0.82	412.43

propose five possible structures with the different substituted sites for the other Fe atom in the $C_{59}Fe$ cage. They are: (1) on the Fe cross site of the hexagonal ring ($C_{58}Fe_2$-1), (2) the site nearest to Fe in a pentagonal ring ($C_{58}Fe_2$-2), (3) the site contributing the most to the LUMO of $C_{59}Fe$ ($C_{58}Fe_2$-3), (4) the site contributing the most to the HOMO of $C_{59}Fe$ ($C_{58}Fe_2$-4), and (5) on the Fe opposite side of the cage ($C_{58}Fe_2$-5).

Table 1 gives HOMO, LUMO, the energy gap between HOMO and LUMO (E_g), and binding energy (BE) of above five isomers, and C_{60} and $C_{59}Fe$ for comparison. Commonly, the thermodynamic stability of a fullerene is determined by BE [22], which is defined as the absolute value of the difference between the total energy of the molecule and the energy sum of all free atoms constituting the molecule. It is obvious from the table that $C_{58}Fe_2$-3 is the most thermodynamically stable. Therefore, the DFT calculations confirm the prediction of FOT. On the other hand, the calculated BE of $C_{59}Fe$ is 5.36 eV smaller than that of C_{60}, while $C_{58}Fe_2$-3 is 4.86 eV smaller than that of $C_{59}Fe$, indicating that the energy required for replacing the second carbon is less than that for replacing the first carbon in the C_{60} network. Thus, we believe that the second carbon can be substituted by the other Fe atom in $C_{59}Fe$ to form a cage $C_{58}Fe_2$.

We next give the analysis of bond lengths for $C_{59}Fe$ and $C_{58}Fe_2$-3. Our calculations show that all C-C bond lengths for $C_{59}Fe$ are in the range from 1.40 to 1.48 Å while Fe-C bond lengths are 1.81 Å, and 1.88 Å, which are 29.3% and 28.8% longer than the original double bonds 1.40 Å and single bonds 1.46 Å of C_{60} respectively. For $C_{58}Fe_2$-3, four Fe-C bond lengths are equal 1.89 Å, which are shorter than the sum of the radius of Fe and that of C 2.01 Å. The Fe=Fe bond of $C_{58}Fe_2$-3 upheaves with an elongated bond length 2.12 Å, which is about 51% longer than its parent's C=C bond. However, it is 1.70 Å smaller than the distance between the two Fe atoms in the free Fe_2 cluster calculated by us, implying that the shortened distance between two Fe atoms in $C_{58}Fe_2$-3 may cause spin quenching of Fe atom to some extent. On the other hand, all C-C bond lengths change very little, indicating that the deformation of the cage resulted from the replacement of two Fe atoms is confined in the local environment of the Fe=Fe bond.

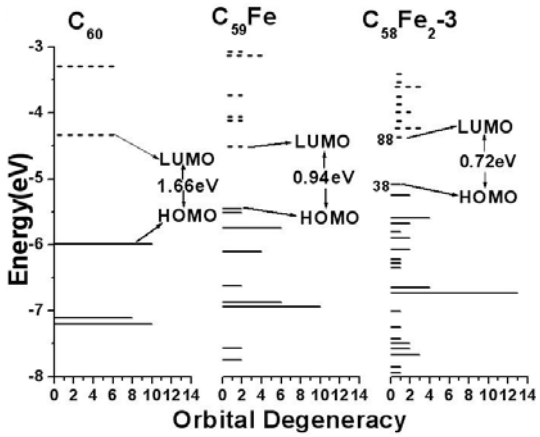

Fig. 3. The energy levels of C_{60}, $C_{59}Fe$, and $C_{58}Fe_2$-3.

3.3 The electronic properties of $C_{58}Fe_2$-3

Figure 3 shows the energy levels of $C_{58}Fe_2$-3 and $C_{59}Fe$ together with that of C_{60} for comparison. The molecular orbitals whose energies agree with each other within a difference of 0.05 eV are regarded as degenerate. The length of the horizontal bar shows the orbital degeneracy. The broken line stands for unoccupied orbital, while the solid line stands for occupied orbital. The contributions from Fe atom states to HOMO and LUMO are marked in terms of percentage of population next to the levels for $C_{58}Fe_2$-3. We define the Fermi level as the half between HOMO and LUMO. It can be seen from the figure that the HOMO and LUMO of $C_{58}Fe_2$-3 contain 38% and 88% Fe character respectively, thus the electron attachment and detachment should occur at the doped Fe sites and the carbon sites of the cage respectively. Furthermore, we compare the E_g of all the considered structures, because they are often correlated with the kinetic stabilities [23,24]. The E_g of $C_{58}Fe_2$-3 is only 0.22 eV smaller than that of $C_{59}Fe$, but is 0.095 eV larger than that of $C_{58}Si_2$ [25], and 0.15 eV larger than that of $C_{58}N_2$ and $C_{58}B_2$ [26]. It is also 0.21 eV, 0.57 eV, 0.54 eV, and 0.48 eV larger than that of $C_{59}Co$ [27], $C_{59}Ni$ [27], $C_{59}Rh$ [27], and $C_{59}Sm$ [28] respectively. Therefore, we think that the kinetic stability of $C_{58}Fe_2$-3 can be comparable to many isolated substituted fullerenes.

In order to explore the electronic structure in a wider range, the total density of states (TDOS) for $C_{58}Fe_2$-3 and C_{60}, and the partial densities of states (PDOS) for Fe_2 in $C_{58}Fe_2$-3 are plotted in Figure 4. The DOS is obtained by a Lorentzian extension of the discrete energy levels with weights being the orbital populations in the levels, and a summation over them. The broadening width parameter is chosen to be 0.15 eV and the Fermi level (E_f) is taken as zero. For the PDOS of Fe_2, many sharp peaks are observed in the energy range from -10 to 0 eV, revealing the strong hybridization between the atomic orbitals of Fe atom and those of the carbons of the cage, which lead to the spin quenching of Fe atom in $C_{58}Fe_2$-3.

The Mulliken charge of Fe atom in $C_{58}Fe_2$-3 shows that the two Fe atoms of $C_{58}Fe_2$-3 lose 0.70 electron to

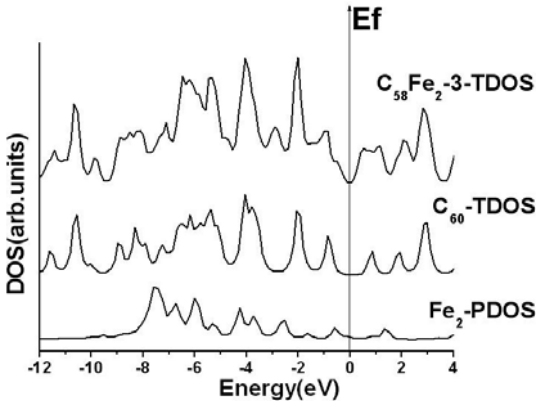

Fig. 4. The TDOS of C_{60} and $C_{58}Fe_2$-3, and the PDOS of Fe_2 in $C_{58}Fe_2$-3.

the carbons of the cage. The net spin population analysis indicates that each Fe atom has 1.11 μ_B magnetic moments, while each of the four nearest neighboring carbons has -0.064 μ_B magnetic moments, and each of the other carbons has less than 0.01 μ_B magnetic moments. Thus, the two Fe atoms have ferromagnetic interaction with each other, and have weak antiferromagnetic interaction with their four nearest neighboring carbons, leaving 2.0 μ_B magnetic moments for the molecule.

4 Conclusion

The formation mechanism, geometric structures, and electronic properties of metal-substituted fullerene $C_{58}Fe_2$ have been studied using FOT and DFT. FOT predicts that two Fe atoms prefer to substitute the carbons of a [6,6] double bond of C_{60}, which is different from the opposite substitution sites of the cage or in the nearest neighboring sites of a pentagonal ring for $C_{58}X_2$ (X = N and B), and also different from the cross sites of a hexagonal ring for $C_{58}Si_2$. Among the five different isomers of $C_{58}Fe_2$, the most stable structure is in a good agreement with the prediction of FOT. The DOS analysis shows that there is a strong hybridization between the atomic orbitals of Fe atom and those of the carbons, leading to the spin quenching of Fe atom in $C_{58}Fe_2$-3. The Mulliken charge of Fe atom in $C_{58}Fe_2$-3 shows that the two Fe atoms of $C_{58}Fe_2$-3 lose 0.70 electron to carbons of the cage. The net spin population analysis indicates that each Fe atom has 1.11 μ_B magnetic moments, while each of the four nearest neighboring carbons has -0.064 μ_B magnetic moments, and each of the other carbons has less than 0.01 μ_B magnetic moments. Thus, the two Fe atoms have ferromagnetic interaction with each other, and have weak antiferromagnetic interaction with their four nearest neighboring carbons, leaving 2.0 μ_B magnetic moments for the molecule.

This work is partially supported by the National Natural Science Foundation of China (Grant No. 10174039), the Natural Science Foundation of Jiangsu Province (Grant No. BK2002099 and BK2006204).

References

1. A.F. Hebard, M.J. Rosseinsky, R.C. Haddon, D.W. Murphy, S.H. Glarum, T.T.M. Palstra, A.P. Ramirez, A.R. Kortan, Nature **350**, 600 (1991)
2. R.H. Xie, Phys. Lett. A **258**, 51 (1999)
3. W. Branz, I.M.L. Billas, N. Malinowski, F. Tast, M. Heinebrodt, T.P. Martin, J. Chem. Phys. **109**, 3425 (1998)
4. T. Guo, C.M. Jin, R.E. Smalley, J. Phys. Chem. **95**, 4948 (1991)
5. R.G. Yu, M.X. Zhan, D.D. Cheng, S.Y. Yang, Z.Y. Liu, L.S. Zheng, J. Phys. Chem. **99**, 1818 (1995)
6. T. Kimura, T. Sugai, H. Shinohara, Chem. Phys. Lett. **256**, 269 (1996)
7. J.L. Fye, M.F. Jarrold, J. Phys. Chem. A **101**, 1836 (1997)
8. I.M.L. Billas, W. Branz, N. Malinowski, F. Tast, M. Heinebrodt, T.P. Martin, C. Massobriot, M. Boerott, M. Parrinello, Nanostruct. Mat. **12**, 1071 (1999)
9. T.G. Schmalz, W.A. Seitz, D.J. Klein, G.E. Hite, J. Am. Chem. Soc. **110**, 1113 (1988)
10. Z.F. Chen, K.Q. Ma, Y.M. Pan, X.Z. Zhao, A.C. Tang, Can. J. Chem. **77**, 291 (1999)
11. N. Kurita, K. Kobayashi, H. Kumahora, K. Tago, Phys. Rev. B **48**, 7 (1993)
12. I.M.L. Billas, C. Massobrio, M. Boero, M. Parrinello, W. Branz, F. Tast, N. Malinowski, M. Heinebrodt, T.P. Martin, J. Chem. Phys. **111**, 6787 (1999)
13. H.P. Wu, K.M. Deng, J.L. Yang, Journal of Nanjing university of science and technology **28**, 194 (2004)
14. C.G. Ding, J.L. Yang, Q.X. Li, K.L. Wang, F. Toigo, Phys. Lett. A **256**, 417 (1998)
15. E. Artacho, D. Sànchez-Portal, P. Ordejòn, A. Garcia, J. M. Soler, Phys. Stat. Sol. B **215**, 809 (1999)
16. A.D. Becke, J. Chem. Phys. **88**, 1053 (1988)
17. J.P. Perdew, Y. Wang, Phys. Rev. B **45**, 13244 (1992)
18. P. Hohenberg, W. Kohn, Phys. Rev. **136**, 864 (1964); W. Kohn, L.J. Sham, Phys. Rev. **140**, 1133 (1965)
19. R. Fletcher, *Practical Methods of Optimization* (Wiley, New York), Vol. 1, 1980
20. K. Fukui, Acc. Chem. Res **4**, 57 (1971)
21. W. Branz, I.M.L. Billas, N. Malinowski, F. Tast, M. Heinebrodt, T.P. Martin, J. Chem. Phys. **109**, 3425 (1998)
22. G.Y. Sun, M.C. Nicklaus, R.-H. Xie, J. Phys. Chem. A **109**, 4617 (2005)
23. J.I. Aihara, Theo. Chem. Acc. **102**, 134 (1999)
24. J.I. Aihara, Chem. Phys. Lett. **343**, 465 (2001)
25. I.M.L. Billas, F. Tast, W. Branz, N. Malinowski, M. Heinebrodt, T.P. Martin, M. Boeroa, C. Massobriob, M. Parrinello, Eur. Phys. J. D **9**, 337 (1999)
26. S.H. Wang, F. Chen, Y.C. Fan, M. Kashni, M. Malaty, S.A. Jansen, J. Phys. Chem. **99**, 6801 (1995)
27. C.G. Ding, J.L. Yang, X.Y. Cui, C.T. Chan, J. Chem. Phys. **111**, 8481 (1999)
28. G.L. Lu, K.M. Deng, H.P. Wu, J.L. Yang, X. Wang, J. Chem. Phys. **124**, 54305 (2006)